

1 This is a non-peer reviewed manuscript draft by Cody Mason

2

3 **Comparison of U-Pb detrital zircon signatures across sediment routing system segments:**
4 **insights from the late Pleistocene Mississippi River and deep-sea fan**

5

6 *^aCody C. Mason, ^aJourdan W. Speessen, ^aJack Heltzer, ^aG. Paul Miles II, ^bBrian W. Romans,
7 ^dDaniel F. Stockli, ^cMike Blum, and ^eAndrea Fildani

8

9 ^aDepartment of Geosciences, University of West Georgia, 1601 Maple St, Carrollton GA 30118

10 ^bDepartment of Geosciences, Virginia Tech, 4044 Derring, Blacksburg VA, 24061

11 ^cDepartment of Geology, University of Kansas, 475 Jayhawk Blvd Lawrence, KS 66045

12 ^dDepartment of Geological Sciences, Jackson School of Geosciences, University of Texas at
13 Austin

14 ^eThe Deep Time Institute, P.O. Box 27552, Austin, Texas 78755-7552, U.S.A.

15

16 *corresponding author email: cmason@westga.edu

17

18

19

20

21

22

23

24 **Abstract:**

25 The Pleistocene Mississippi sediment routing system has experienced significant
26 drainage reorganizations in response to Northern Hemisphere glaciation. Geologically recent
27 (<25 ka) and large (~90 km) river avulsions have occurred in the Mississippi's lower alluvial
28 valley, yet whether these punctuated autogenic phenomena influenced down system records of
29 sedimentary provenance is unknown. We present U–Pb detrital zircon (DZ) geochronology from
30 near last glacial maximum (LGM; ~25 ka) and early deglacial (~14 ka) aged fluvial deposits of
31 the Mississippi Valley, United States, integrated with published DZ samples from the Gulf of
32 Mexico (Mississippi fan), to show a high similarity of DZs from late Pleistocene fluvial deposits
33 and those from time correlative deep-marine deposits. These results imply the last glacial
34 Mississippi River efficiently transferred DZs from river to deep-sea with little modification to
35 the riverine DZ signature. Stratigraphically deeper DZ samples in the Mississippi fan contain
36 distinct DZ age spectra, which likely represent the primary DZ signature of the Mississippi
37 between isotope (MIS) stages 5 – 3. Mixture modeling of DZ samples recovered from late
38 Pleistocene (MIS-2) deposits in the Western Lowlands and Eastern Lowlands of the Mississippi
39 Valley suggests ~80% of the DZs in a LGM-to-deglacial Mississippi River were sourced from
40 the glacial Missouri River, with lesser but appreciable contributions from the glacial Upper
41 Mississippi River (13 – 20%). Only minute contributions of DZs are interpreted from the glacial
42 Arkansas (1 – 5%) and Ohio Rivers (0 – 2%). Given the interpreted lack of Ohio river derived
43 DZs in the Western Lowlands at ca. 25 ka, we suggest a glacial Ohio river did not join a
44 combined Missouri-Mississippi River at the sampled location in the Western Lowlands at ~25,
45 and may or may not have joined the Missouri-Mississippi in the Eastern Lowlands at ~15 ka.
46 Our geochronological analyses included several grain size fractions for each sample location; a

47 lack of Gondwanan-Appalachian aged DZs in one sub sample grain size fraction illustrates the
48 need for mineral separation methods and U-Pb age measurement methods that include all
49 available size fractions, or risks serious error in provenance interpretations.

50

51 **Introduction:**

52 The manner in which climate change, tectonic perturbations, or autogenic sedimentary
53 phenomena influence sediment supply magnitude, grain size, and sediment supply rate to basins
54 is crucial knowledge when attempting to decode stratigraphic patterns (Dickinson, 1974;
55 Jerolmack and Paola, 2010; Allen and Allen, 2013; Allen et al., 2016; Romans et al., 2016;
56 Jonell et al., 2018; Straub et al., 2020). An equally important aspect of deciphering upstream
57 environmental changes from stratigraphy is the potential for changes in sediment source areas as
58 inferred from detrital minerals (Weislogel et al, 2006; Gehrels, 2014; Sharman et al., 2019).
59 Indeed, constraining the sources of sediment preserved in basins using sedimentary provenance
60 has become an integral component to studies which attempt to decode paleogeography or invert
61 past external forcings from ancient sedimentary deposits (Thomas, 2011; Lawton, 2014;
62 Caracciolo, 2020). Furthermore, studies of sedimentary provenance in modern- to sub-modern
63 sedimentary systems — those systems much older than historical records, but for which past
64 drainage basin configurations may be fairly well constrained (e.g. Sømme et al., 2009) — when
65 combined with published tectonic and climatic records and direct observations, have allowed
66 geoscientists to refine how deep-time boundary conditions may have influenced stratigraphic
67 archives (Mason and Romans, 2018; Blowick et al., 2019; Malkowski et al., 2019; Blum et al.,
68 2018; Capaldi et al., 2019; Sickman et al., 2016; 2019; Mason et al. 2019; Fildani et al., 2018;
69 Hessler et al., 2018).

70 Sediment routing systems move sediment and solutes across Earth's surface, generally
71 from upland regions of sediment production, to adjacent sedimentary basins (Allen, 2008; Sinha,
72 2011). Studies of sedimentary basins often rely on sedimentologic and stratigraphic data from
73 only one system segment, leaving open the prospect for unrecognized effects of grain size
74 fractionation or autogenic sediment recycling along depositional dip of the sediment routing
75 system (Pettit et al., 2019). For example, differential preservation and/or lack of access to
76 outcrops or cores in subsiding or ancient sedimentary basins often precludes direct comparisons
77 of sedimentary provenance across time correlative system segments. The Mississippi River to
78 deep-sea fan system (Fig. 1 A) is a globally significant sediment routing system, has been well-
79 studied since the mid 1900s (Fisk, 1944; Saucier, 1986; Bentley et al., 2016; Fildani et al., 2016;
80 Blum, 2019), and is composed of relatively well-dated and relatively accessible deposits in the
81 fluvial (Rittenour et al., 2007) and marine environments (Bouma et al., 1986; Fildani et al.,
82 2016). The Mississippi sediment routing system has revealed numerous insights about the
83 manner in which climatic histories of North America have impacted the sedimentary record and
84 preservation of its fluvial systems (Saucier, 1994; Blum, 2000; Counts et al., 2015), the
85 architecture of deep-sea fans (Bouma, 1986; Bentley et al., 2016), and global climate through the
86 flux of glacial meltwater to Earth's oceans (Licciardi et al., 1999; Aharon, 2003). One significant
87 finding is that ice sheet growth and decay may have modified the sources of riverine sediment
88 input to the Mississippi fan over the last glacial-interglacial period (Mason et al., 2017; Fildani et
89 al., 2018). However, the nature of the apparent changes in sediment sources, as preserved in the
90 deep-sea, are not well constrained and thus merit further investigation.

91 In this paper we present new detrital zircon U-Pb geochronology (N = 6 samples, n = 742
92 individual U-Pb ages), and integrate these new results with abundant existing DZ geochronology

93 from the Modern Mississippi River and its tributaries (Blum and Pecha, 2014), and the
94 Mississippi deep-sea fan (Fildani et al., 2016; Mason et al., 2017; Fildani et al., 2018). We
95 interpret these DZ age spectra across the fluvial to marine zones in the context of potential
96 allogenic forcings (e.g. ice sheet fluctuations) and autogenic forcings along depositional dip (*e.g.*
97 large river avulsions, sediment recycling and or mixing in the coastal to marine zone).

98

99 **Study Area and Methods**

100 The Mississippi sediment routing system (Fig. 1 A) consists of an onshore,
101 transcontinental fluvial network, a large subaerial delta positioned at the edge of the continental
102 shelf in the Gulf of Mexico, a submarine canyon system active during glacioeustatic lowstands,
103 and a deep-sea fan consisting of accumulations of mainly terrigenous sediment (Fig. 1 A-B). The
104 onshore Mississippi fluvial system has experienced significant modifications since the onset of
105 northern hemisphere glaciations (Carson et al., 2018). Between > 65 ka to 25 ka, the course of
106 the Missouri – Upper Mississippi Rivers likely followed a path through the Western Lowlands,
107 west of Crowley’s Ridge (Fig. 1) in the Mississippi Valley (Rittenour et al., 2007; Blum 2019).
108 After ~25 ka the Mississippi – Missouri River avulsed east into the Eastern Lowlands. The
109 course of the glacial Ohio River may or may not have joined the main trunk Mississippi in the
110 western lowlands, and similarly is unconstrained in space and time in the eastern Lowlands
111 (Blum, 2019). Deep-sea sediment deposited between approximately 65 – 11 ka records large
112 fluctuations in the relative proportions of DZs from the Ohio and Mississippi-Missouri Rivers
113 (Fildani et al., 2018). Sediment aged ~25 to 15 ka in the Mississippi Valley may hold clues to the
114 complex and most recent avulsion history.

115 The modern Missouri River supplies the majority (>40 – 50%) of suspended sediment to
116 the main stem Mississippi River and delta (Heimann et al., 2011), and likely was more
117 significant in terms of relative sediment loads in the pre-dam historical period. Past the limit of
118 instrumental and historical records, U-Pb DZ provenance of sands from ancient deposits may be
119 used to constrain sediment source areas (Blum and Pecha, 2014), as well as changing relative
120 sediment loads through time (Mason et al., 2017). Specifically, Mason et al. (2017) identified a
121 strong similarity between measured relative suspended sediment loads of tributaries to the
122 Mississippi, and the results of quantitative DZ top-down mixing models (e.g. Sharman and
123 Johnstone, 2017). Mason et al. (2017) concluded that a full glacial Missouri River supplied
124 greater amounts of DZs (>70 – 90% of total) to the deep-sea fan than the river supplies to the
125 modern fluvio-deltaic zone (~60 – 70% of total), which is consistent with historical accounts of
126 sediment loads before anthropogenic modifications to the Missouri River.

127 Relatively high proportions of Western Cordillera aged DZs (0 – 280 Ma) in MIS-2 aged
128 deep-sea deposits (Fig. 2) support an interpretation that the refractory detrital composition of the
129 Mississippi fan is largely sourced from drainage basins in the western United States. The relative
130 proportions of DZ age spectra change in a systematic way through stratigraphically older
131 portions of the Mississippi fan, suggesting that sediment sources were more equally partitioned
132 between eastern, northern, and western regions of the drainage basin—e.g. the Ohio River,
133 Upper Mississippi River, and Missouri River, respectively, before the LGM (Fig. 2; Fildani et
134 al., 2018). Taken together, DZs from the deep-sea fan and the modern fluvio-deltaic system
135 segment fingerprint sediment sources, and tell a story of changing detrital mixtures, interpreted
136 as changing source areas or relative sediment loads in the ancient Mississippi catchment through
137 time. To summarize these observations, interglacial to early glacial climates appear to be

138 associated with deposits containing higher proportions of eastern-derived DZs, whereas full
139 glacial climates appear to be associated with deposits containing higher proportions of western-
140 and northern-derived DZs. The record of detrital mixtures for the fluvial realm across the Late
141 Pleistocene is largely unconstrained, but may yield insights into the functioning of the
142 sedimentary system across glacial-interglacial cycles.

143 In order to interrogate DZ signatures of the ancient fluvial archive, we collected samples
144 from the Western and Eastern Lowlands of the Central Mississippi Valley (Fig. 1 B). We used a
145 sediment vibrocore and a power auger to recover late Pleistocene river sands buried beneath
146 several meters of late Pleistocene to Holocene soil and loess deposits (See Fig. 3 A – C for
147 surface morphology at sample locations).

148 Sampling was guided by the published optically stimulated luminescence (OSL)
149 chronology of Rittenour et al. (2007), and the published dissertation (2004) that contains detailed
150 sedimentologic descriptions for each OSL sample location (noted below). The site of sample
151 MV01 (this study) is located in the Western Lowlands, west of Crowley's Ridge, and was
152 collected from the 24.6 ± 1.8 ka Ash Hill fluvial braid belt (Fig. 1 B for location). At this
153 location, Rittenour described the Peoria loess from a depth of 0 – 220 cm, and fine to medium
154 grained sand below 220 cm depth (sample 125). Sample MV01 was collected from below the
155 Peoria loess at a depth of ~250 cm, and consisted of relatively clean, fine to medium grained
156 sands (Fig. 3 D).

157 The site of sample MV03 (this study) is located south of- and east of Crowley's Ridge, in
158 the Eastern Lowlands of the central Mississippi Valley, and was collected from the 14.7 ± 1.1 ka
159 Kennett fluvial channel belt (Fig. 1 B). Rittenour (2004) described silty clay, interpreted as
160 natural levee deposits, from 0 – 140 cm, underlain by oxidized to unoxidized medium to coarse

161 sands from 140 – >240 cm depth (sample 122). Sample MV03 was collected beneath thicker
162 loess and levee deposits at a depth of ~330 – 340 cm, and consisted of silty very fine to medium
163 grained sand (Fig. 3 D).

164 Grain size is known to influence DZ age distributions in fluvial environments such as the
165 Rio Orinoco (Ibañez-Mejia et al., 2018), and the Amazon River (Lawrence et al., 2011), yet the
166 influence of grain size on DZ age distributions has not been investigated in the modern or ancient
167 Mississippi River catchment System. We address this using a reconnaissance level sampling
168 strategy. At each sample location we collected one bulk sample of unconsolidated sand from the
169 subsurface. Each bulk sample was later dried, split and then sieved into grain size fractions of
170 <63 μm , 63 – 125 μm , 125 – 250 μm , 250 – 500 μm , and >500 μm (see Table 1, Fig 2 D). A total
171 of six sub samples were processed for extraction of DZs — the bulk sediment for each sample,
172 the 63 – 125 μm , and the 125 – 250 μm fraction from samples MV01 and MV03.

173 We applied standard mineral separation techniques to samples of bulk sediment and grain
174 size splits at the UTChron facility, University of Texas at Austin (USA), following the
175 procedures of Thomson et al. (2017). After separation of zircons, U-Pb ages were measured
176 using laser ablation–inductively coupled plasma–mass spectrometry. Of the subsample grain size
177 fractions, insufficient amounts of DZs were recovered from the >250 μm size fractions to
178 perform robust U-Pb geochronology. A data file of full isotopic measurements can be found in
179 the supplementary data file (*this data file will not be available in the preprint version*).

180 In order to guide interpretations of U-Pb geochronologic results, we applied a statistical
181 mixing model (after Fildani et al., 2018; Mason et al., 2019) to define the most likely sources of
182 DZs to downstream sedimentary deposits in the Western and Eastern Lowlands between ~25 –
183 15 ka. In this method of unmixing DZ samples, DZs from Pleistocene fluvial samples represent a

184 daughter composite mixture that we assume to be derived completely from several representative
185 parent components—DZ samples collected from modern sands of the major tributaries to the
186 Mississippi River (Blum and Pecha, 2014). We used a Monte Carlo approach to forward model
187 2e6 random combinations of parent components, and select the best fit model by minimizing the
188 areal mismatch between observed daughter mixture and modeled daughter composite. The
189 calculated relative mixing coefficients should give clues about the relative sediment supply
190 across the LGM to early deglaciation in the Mississippi Valley, and ultimately clues into the
191 ancient river configurations. The unmixing results also serve as a valuable comparisons to
192 similar published quantifications of sediment sources for age correlative deep-sea fan DZ
193 samples (Mason et al., 2017; Fildani et al. 2018).

194

195 **Results**

196 Individual DZ U-Pb age spectra for each bulk sample and each subsample are plotted as
197 kernel density estimates (KDEs) and cumulative distribution functions in Figure 4 (using
198 detritalPy; Sharman et al., 2018). These results show a subtle, systematic variation in DZ age
199 spectra between bulk grain size, and subsamples of MV01 and MV03. In general, sample MV01
200 (Western Lowlands; 25 ka) is characterized by higher proportions of Trans-Hudson/Penokean
201 and Wyoming/Superior aged DZs (>1800 Ma), and relatively low proportions of Appalachian-
202 Gondwanan aged DZs (280 – 800 Ma). Sample MV01 contains a greater proportion of Jurassic
203 aged DZs, as compared to MV03. Sample MV03 (Eastern Lowlands; 15 ka) is characterized by a
204 greater proportion of Appalachian-Gondwanan aged DZs, and lower proportions of Trans-
205 Hudson/Penokean and Wyoming/Superior aged DZs.

206 Overall, there appears to be no systematic variation in DZ age spectra with respect to
207 grain size for each sub sample group, with the exception of subsample MV01 125 – 250 μm size
208 fraction. Here we note the complete absence of Appalachian-Gondwanan aged DZs, and a
209 relatively high proportion of Archean DZs as compared to other sub samples from the same
210 deposit. We address this result further in the discussion section.

211 When U-Pb DZ age data for subsamples are amalgamated (Fig. 5), the product is a well-
212 characterized DZ signature of the ancient Mississippi River as it flowed first through the Western
213 Lowlands around 25 ka, and later through Eastern Lowlands around 15 ka. Unmixing the
214 amalgamated DZ samples from the Western Lowlands results in mixing coefficients strongly
215 partitioned between the Missouri River (79%), and the Upper Mississippi River (21%) (Fig. 6 C;
216 Table 1). Unmixing DZ samples from the Eastern Lowlands results in mixing coefficients
217 weighted toward the Missouri (80%), Upper Mississippi (13%), and lesser values for
218 contributions from the Arkansas River (5%), and minimal values for contributions from the Ohio
219 River (2%) (Fig. 6 D).

220

221 **Discussion**

222 New DZ age data from late Pleistocene deposits of the Mississippi fluvial system offer
223 insights into sediment sources during the LGM through early deglacial conditions in the
224 Mississippi fluvial system, a time of significant environmental change and major river avulsions
225 in the Mississippi River Valley. Qualitatively, fluvial DZ samples resemble a mixture of the
226 modern Missouri River, and the Upper Mississippi River, while also strongly resembling DZ
227 samples from time correlative Mississippi deep-sea fan sediment (Fig. 5). These results suggest a
228 robust link between river and deep-sea fan.

229 To better interpret the potential sediment sources, and to quantitatively visualize the
230 similarity of each sample's age spectra, we plotted existing DZ age data for the largest modern
231 tributaries to the Mississippi River (from Blum and Pecha, 2014; presented in Mason et al.,
232 2017) and the new DZ age data on a multidimensional scaling map (MDS map; after Vermeesch,
233 2013) (Fig. 7). The resulting Euclidean distances between samples on the MDS map show the
234 Ohio River is relatively dissimilar to MIS-2 Pleistocene fluvial samples and to the MIS-2 aged
235 deep-sea samples. The MDS map indicates a close similarity of LGM fluvial samples to the
236 modern Missouri River, and to a lesser degree the Upper Mississippi River. Mixing models agree
237 with, and reinforce interpretations made from the MDS map. Given the strong similarity between
238 previous mixing model results and measured relative sediment supply in the modern Mississippi
239 system, it is likely these new model results offer a glimpse into the ice age relative sediment
240 loads of the Mississippi River (Fig. 8). Mixing coefficients for sample MV01 suggest the
241 Missouri River and Upper Mississippi supplied most or nearly all of the sediment to the Ash Hill
242 braid belts in the Western Lowlands at ~25 ka, and neither the Arkansas nor the Ohio Rivers
243 contributed quantifiable proportions of DZs to this location at that time.

244 After 25 ka, the Missouri – Mississippi River avulsed into the Eastern Lowlands through
245 the Bell City Oran Gap (Fig. 8; Rittenour et al., 2017). It would seem plausible, or perhaps likely
246 the DZ signature in the Eastern Lowlands would be influenced by the glacial Ohio River with its
247 abundant Grenville and Appalachian-Gondwanan DZs. However, this prediction is not borne out
248 by the DZ distributions from sample MV03. The samples from the eastern lowlands do not
249 contain the strong Grenville DZ signature which could be related to the modern Ohio River, yet
250 do contain abundant Western Cordillera aged DZs. Early deglacial aged Kennett channel belts
251 (~14 ka) of the central/Eastern Lowlands contain less Archean and Jurassic DZs (northern and

252 western signatures, respectively), and slightly more Appalachian-Gondwanan DZs (eastern
253 signature). Bulk samples and subsamples of MV03 plot closest to the MIS-2 deep sea fan
254 samples in MDS space (Fig. 7). Furthermore. These samples, like those of MV01, cluster nearest
255 the modern Missouri River in MDS space. Mixing coefficients for sample MV03 suggest the
256 Missouri River supplied about the same proportion of DZs to the Eastern Lowlands at 15 ka
257 (80%), while the Upper Mississippi and Arkansas also contributed moderate amounts of DZs,
258 and the Ohio River supplied scarcely quantifiable amounts of DZs to this location in the Eastern
259 Lowlands at ~15 ka. Our results and interpretations suggest that sediment supply from the
260 Missouri River was dominant in all segments of the Mississippi system between the fluvial
261 valley and deep-sea fan during the immediate lead up to the LGM through early deglaciation
262 (Fig. 8).

263 While mixing model results suggest that a glacial Ohio River may not have contributed
264 DZs to the main trunk Mississippi at 15 ka, that scenario—where the hydrologically largest
265 tributary was dammed by ice, or flowed parallel to, but apart from the Mississippi in the Eastern
266 lowlands at 15 ka—may be overly simplistic. One plausible explanation for an apparent lack of
267 glacial Ohio River derived DZs might be the relative erodibility of substrate in western vs.
268 eastern drainage basins. For example sedimentary substrates in the Missouri River basin and the
269 Great Plains could have supplied abundant Mesozoic through Cenozoic aged clastic sediment to
270 the system, while eastern substrates, carved by the Ohio River, are composed of dominantly
271 resistant Paleozoic strata, and simply eroded more slowly providing less clastic sediment to the
272 Mississippi river system. The glacial till from northern and western basins could have enhanced
273 the amount Western Cordillera DZs and account for relatively low proportions of eastern sourced
274 DZs. However, Mason et al (2017) quantified ~14 – 17% contributions of Ohio derived DZs in

275 modern lower Mississippi River sediment, which suggests relative erodibility alone may not
276 explain the lack of apparent Ohio-derived DZs. Another plausible explanation is that
277 geographically variable climatic conditions (temperature, hydroclimate) across the Mississippi
278 catchment modulated erosion rates over late Pleistocene to Holocene timescales, as proposed for
279 the Trinity, Brazos, and Colorado Rivers of Texas (Hidy et al., 2014), and the continent scale
280 Amazon River catchment (Mason et al., 2019).

281 The potential for grain size to influence interpretations of sediment provenance is
282 illustrated by the DZ age spectra of subsample MV01 (125 – 250 μm). If the fine sand sized
283 subsample from MV01 were the only provenance data available for a given sedimentary basin,
284 one would be forced to interpret a complete lack of Appalachian-Gondwanan sourcing in its
285 upstream catchment — an unlikely phenomenon for large rivers of central or eastern North
286 America (Dickinson, 2009; Blum and Pecha, 2014), nor deposits from ancient sedimentary
287 basins of western North America, all of which which tend to incorporate recycled Grenville and
288 older DZ populations (Schwartz et al., 2019). One logical explanation for a lack of Appalachian
289 DZs in the 125 – 250 μm fraction of MV01, is that Appalachian and Gondwanan aged zircons
290 tend to be smaller, and that Archean zircons found in abundance in other subsample size
291 fractions tend to be larger. This result may merit further investigation but is out of the immediate
292 scope of this work. However, given the initial result of analyses of grain size fractions in the
293 Mississippi sediment routing system, we advocate for the inclusion of all grain size fractions
294 when performing mineral separations for DZ provenance analysis.

295 The relatively high abundance of late Cretaceous DZs in all existing samples from the
296 late Pleistocene Mississippi sediment routing system is an unexplained phenomenon. Fildani et
297 al. (2016) proposed enhanced sediment supply from the Rocky Mountains of the American west

298 (and perhaps the Canadian Rockies), driven by large glacial outburst floods, and an associated
299 increase in the supply of glacial till rich in western derived detritus. The DZ distributions of
300 newly sampled Pleistocene fluvial deposits contain an abundance of late Cretaceous DZs, which
301 is consistent with the interpretation of Fildani et al. (2016). Similar high proportions of Western
302 Cordillera DZs in fluvial sediments and age correlative deep-sea fan sediments argue against
303 grain size fining as a primary control on this age populations.

304 Pleistocene fluvial deposits in the Western and Eastern Lowlands are dominated by
305 supply from the ancestral Missouri River, and to a lesser degree the Upper Mississippi River, as
306 are the deep-sea deposits of MIS-2 age in the Mississippi fan. The similarity of late Pleistocene
307 fluvial DZ samples to time correlative DZ samples from the deep-sea fan supports the concept of
308 rapid signal propagation through a glacial to early deglacial continent scale river to fan system,
309 during glacioeustatic lowstand. Here, we have shown again that deep-sea fans are faithful
310 recorders of continent scale catchments (Fildani and Hessler, 2019). The application of relatively
311 high resolution sampling across sediment routing system segments in the Mississippi River and
312 fan contributes to the growing body of work that posits sediment sources in the fluvial segment,
313 and as recorded in deep-sea fans, are sensitive to climatic and ice sheet controlled forcings over
314 Milankovitch timescales. A novel result of this work is that DZ provenance of deposits from the
315 late Pleistocene river and fan appear less sensitive to the relatively large river avulsions
316 documented between ~25 – 15 ka in the Mississippi Valley, than to overall system-wide external
317 forcing of climate change and associated ice sheet growth and decay throughout the Pleistocene.

318

319 **Conclusions**

320 We applied U-Pb detrital zircon (DZ) geochronology to late Pleistocene fluvial deposits
321 of the Mississippi Valley to investigate the sources of sediment in the Mississippi sediment
322 routing system just prior (25 ka) to the last glacial maximum (LGM) and during early
323 deglaciation (15 ka). We find the Missouri-Mississippi River dominated DZ supply at all
324 observed periods of time, and found no evidence from the DZ record of the glacial Ohio River
325 contributing significant quantities of sediment or DZs the Mississippi River or deep-sea fan. The
326 age spectra from bulk sediment samples and sub samples from the late Pleistocene fluvial system
327 presented here agree with the existing hypothesis that a combined Missouri – Upper Mississippi
328 River once flowed through the Western Lowlands of the Mississippi Valley, west of Crowley’s
329 Ridge, and was separate from the Ohio River at ~25 ka. After 25 ka, this river system avulsed
330 into the Eastern Lowlands through the Bell City – Oran Gap, and later through Thebes Gap,
331 where downstream DZ sample age spectra and mixture modeling results are inconsistent with
332 contributions of DZs from an early deglacial Ohio River. The strong similarity of late
333 Pleistocene fluvial DZs to published DZ samples from the LGM to deglacial Mississippi deep-
334 sea fan suggests that no significant modifications of DZ mixtures occurred en route to the deep-
335 sea fan, and confirms that fans are robust recorders of their continental drainage basins. Our
336 preliminary analyses of DZ ages across grain sizes, and the similarity of those sample age spectra
337 to samples of the LGM deep-sea fan, suggests that down system grain size fining may not play a
338 major role in the age populations found in deep sea environments in the Gulf of Mexico. The
339 large autogenic river avulsions experienced by the Mississippi-Missouri River across ~25 – 15
340 ka did not significantly influence the downstream fluvial DZ signature of the glacial Mississippi
341 River, nor those of deposits measured in the deep sea fan. First order controls on detrital
342 mixtures in the Mississippi River to fan system appear to be tectonic-induced relief, and relative

343 erodibility of catchment substrates. Second order controls on detrital mixtures appear to be ice
344 sheet fluctuations that affect sediment source area disproportionately, and variable climatic
345 conditions across the Mississippi catchment, such as temperature, hydroclimate, and glacially
346 modified hydrology of major tributaries. Our interpretations are consistent with the idea that
347 older and deeper samples from the Mississippi deep-sea fan, and others fans globally, should also
348 record the primary riverine signature of their ancient terrestrial river segments.

349

350

351

352

353

354

355

356

357

358

359

360

361

362

363

364

365

366 **References**

- 367 Aharon, P., 2003. Meltwater flooding events in the Gulf of Mexico revisited: Implications for
368 rapid climate changes during the last deglaciation. *Paleoceanography* 18, 1–14.
369 doi:10.1029/2002PA000840
- 370 Allen, P.A. & Allen, J.R., 2013. *Basin Analysis: Principles and Application to Petroleum Play*
371 *Assessment*, 3rd edn. Wiley-Blackwell, Oxford.
- 372 Allen, P. A., Michael, N. A., D’Arcy, M., Roda-Boluda, D. C., Whittaker, A. C., Duller, R. A.,
373 and Armitage, J. J., 2016. Fractionation of grain size in terrestrial sediment routing
374 systems. *Basin Research*, p. 1-23.
- 375 Bentley, S.J., Blum, M.D., Maloney, J., Pond, L., Paulsell, R., 2016. The Mississippi River
376 source-to-sink system: Perspectives on tectonic, climatic, and anthropogenic influences,
377 Miocene to Anthropocene. *Earth-Science Rev.* 153, 139–174.
378 doi:10.1016/j.earscirev.2015.11.001
- 379 Blowick, A., Haughton, P., Tyrrell, S., Holbrook, J., Chew, D., Shannon, P., 2019. All mixed up:
380 Pb isotopic constraints on the transit of sands through the Mississippi-Missouri River
381 drainage basin, North America. *Bull. Geol. Soc. Am.* 131, 1501–1518.
382 doi:10.1130/B35057.1
- 383 Blum, M., 2019. Organization and reorganization of drainage and sediment routing through time:
384 The Mississippi River system. *Geol. Soc. Spec. Publ.* 488, 15–45. doi:10.1144/SP488-
385 2018-166
- 386 Blum, M., Pecha, M., 2014. Mid-Cretaceous to Paleocene North American drainage
387 reorganization from detrital zircons. *Geology* 42, 607–610. doi:10.1130/G35513.1

388 Blum, M., Rogers, K., Gleason, J., Najman, Y., Cruz, J., Fox, L., 2018. Allogenic and Autogenic
389 Signals in the Stratigraphic Record of the Deep-Sea Bengal Fan. *Sci. Rep.* 8.
390 doi:10.1038/s41598-018-25819-5

391 Blum, M.D., Törnqvist, T.E., 2000. Fluvial responses to climate and sea-level change: a review
392 and look forward. *Sedimentology* 47, 2–48. doi:10.1046/j.1365-3091.2000.00008.x

393 Bouma, A.H., Coleman, J.M., and Meyer, A.W., 1986, Introduction, objectives, and principal
394 results of Deep Sea Drilling Project Leg 96, in Bouma, A.H., Coleman, J.M., Meyers,
395 A.W., et al., Initial Reports of the Deep Sea Drilling Project, Volume 96: Washington,
396 D.C., U.S. Government Printing Office, p. 15–36, doi: 10.2973/dsdp.proc.96.102.1986.

397 Capaldi, T.N., George, S.W.M., Hirtz, J.A., Horton, B.K., Stockli, D.F., 2019. Fluvial and Eolian
398 Sediment Mixing During Changing Climate Conditions Recorded in Holocene Andean
399 Foreland Deposits From Argentina (31–33°S). *Front. Earth Sci.* 7.
400 doi:10.3389/feart.2019.00298

401 Caracciolo, L., 2020. Sediment generation and sediment routing systems from a quantitative
402 provenance analysis perspective: Review, application and future development. *Earth*
403 *Science Reviews*, <https://doi.org/10.1016/j.earscirev.2020.103226>

404 Carson, E.C., Rawling, J.E., Attig, J.W., Bates, B.R., 2018. Late Cenozoic evolution of the upper
405 Mississippi River, Stream Piracy, and reorganization of north American mid-Continent
406 drainage systems. *GSA Today* 28, 4–11. doi:10.1130/GSATG355A.1

407 Counts, R.C., Murari, M.K., Owen, L.A., Mahan, S.A., Greenan, M., 2015. Late quaternary
408 chronostratigraphic framework of terraces and alluvium along the lower Ohio River,
409 southwestern Indiana and western Kentucky, USA. *Quat. Sci. Rev.* 110, 72–91.
410 doi:10.1016/j.quascirev.2014.11.011

411 Dickinson, W.R., 1974. Plate Tectonics and Sedimentation, in: Tectonics and Sedimentation.
412 doi:10.2110/pec.74.22.0001

413 Fildani, A., Hessler, A.M., Mason, C.C., Mckay, M.P., Stockli, D.F., 2018. Late Pleistocene
414 glacial transitions in North America altered major river drainages, as revealed by deep-sea
415 sediment. *Sci. Rep.* 1–8. doi:10.1038/s41598-018-32268-7

416 Fisk, H.N. 1944. Geological Investigation of the Alluvial Valley of the Lower Mississippi River.
417 War Department, Corps of Engineers, Washington, DC.

418 Gehrels, G., 2014. Detrital Zircon U-Pb Geochronology Applied to Tectonics. *Annu. Rev. Earth*
419 *Planet. Sci.* 42, 127–149. doi:10.1146/annurev-earth-050212-124012

420 Heimann, D.C., Sprague, L.A., and Blevins, D.W., 2011. Trends in suspended-sediment loads
421 and concentrations in the Mississippi River Basin, 1950–2009. U.S. Geological Survey
422 Scientific Investigations Report 2011–5200.

423 Hessler, A.M., Covault, J.A., Stockli, D.F., Fildani, A., 2018. Late Cenozoic cooling favored
424 glacial over tectonic controls on sediment supply to the western Gulf of Mexico. *Geology*
425 46, 995–998. doi:10.1130/G45528.1

426 Hessler, A.M., Fildani, A., 2019. Deep-sea fans: tapping into Earth’s changing landscapes. *J.*
427 *Sediment. Res.* 89, 1171–1179. doi:10.2110/jsr.2019.64

428 Hidy, A.J., Gosse, J.C., Blum, M.D., Gibling, M.R., 2014. Glacial–interglacial variation in
429 denudation rates from interior Texas, USA, established with cosmogenic nuclides. *Earth*
430 *Planet. Sci. Lett.* 390, 209–221. doi:10.1016/j.epsl.2014.01.011

431 Ibañez-mejia, M., Pullen, A., Pepper, M., Urbani, F., Ghoshal, G., Ibañez-mejia, J.C., 2018. Use
432 and abuse of detrital zircon U-Pb geochronology — A case from the Río Orinoco delta ,
433 eastern Venezuela 46, 1–4. doi:10.1130/G45596.1/4508766/g45596.pdf

434 Jerolmack, D.J., Paola, C., 2010. Shredding of environmental signals by sediment transport.
435 *Geophys. Res. Lett.* 37, 1–5. doi:10.1029/2010GL044638

436 Jonell, T.N., Owen, L.A., Carter, A., Schwenniger, J.L., Clift, P.D., 2018. Quantifying episodic
437 erosion and transient storage on the western margin of the Tibetan Plateau, upper Indus
438 River. *Quat. Res. (United States)* 89, 281–306. doi:10.1017/qua.2017.92

439 Lawrence, R.L., Cox, R., Mapes, R.W., Coleman, D.S., 2011. Hydrodynamic fractionation of
440 zircon age populations. *Bull. Geol. Soc. Am.* 123, 295–305. doi:10.1130/B30151.1

441 Lawton, T.F., 2014. Small grains, big rivers, continental concepts. *Geology* 42, 639–640.
442 doi:10.1130/focus072014.1

443 Licciardi, J.M., Teller, J.T., Clark, P.U., 1999. Freshwater routing by the Laurentide Ice Sheet
444 During the Last Deglaciation. *Geophys. Monogr.* doi:10.1029/gm112p0177

445 Malkowski, M.A., Sharman, G.R., Johnstone, S.A., Grove, M.J., Kimbrough, D.L., Graham,
446 S.A., 2019. Dilution and propagation of provenance trends in sand and mud: Geochemistry
447 and detrital zircon geochronology of modern sediment from central California (U.S.A.).
448 *Am. J. Sci.* 319, 846–902. doi:10.2475/10.2019.02

449 Malusà, M.G., Resentini, A., and Garzanti, E., 2016, Hydraulic sorting and mineral fertility bias
450 in detrital geochronology: *Gondwana Research*, v. 31, p. 1–19.

451 Mason, C.C., Fildani, A., Gerber, T., Blum, M.D., Clark, J.D., Dykstra, M., 2017. Climatic and
452 anthropogenic influences on sediment mixing in the Mississippi source-to-sink system
453 using detrital zircons: Late Pleistocene to recent. *Earth Planet. Sci. Lett.*
454 doi:10.1016/j.epsl.2017.03.001

455 Mason, C.C., Romans, B.W., 2018. Climate-driven unsteady denudation and sediment flux in a
456 high-relief unglaciated catchment-fan using ^{26}Al and ^{10}Be : Panamint Valley, California.
457 *Earth Planet. Sci. Lett.* 492, 130–143. doi:10.17605/OSF.IO/5UJRD

458 Mason, C.C., Romans, B.W., Stockli, D.F., Mapes, R.W., Fildani, A., 2019. Detrital zircons
459 reveal sea-level and hydroclimate controls on Amazon River to deep-sea fan sediment
460 transfer. *Geology*. doi:10.1130/G45852.1

461 Pettit, B.S., Blum, M., Pecha, M., McLean, N., Bartschi, N.C., Saylor, J.E., 2019. Detrital-Zircon
462 U-Pb Paleodrainage Reconstruction and Geochronology of the Campanian Blackhawk–
463 Castlegate Succession, Wasatch Plateau and Book Cliffs, Utah, U.S.A. *J. Sediment. Res.*
464 89, 273–292. doi:10.2110/jsr.2019.18

465 Rittenour, T.M., 2004. Fluvial Evolution of the Lower Mississippi Valley over the last Glacial
466 Cycle [PhD dissertation].

467 Rittenour, T.M., Blum, M.D., Goble, R.J., 2007. Fluvial evolution of the lower Mississippi River
468 valley during the last 100 k.y. glacial cycle: Response to glaciation and sea-level change.
469 *Geol. Soc. Am. Bull.* 119, 586–608. doi:10.1130/B25934.1

470 Romans, B.W., Castelltort, S., Covault, J.A., Fildani, A., Walsh, J.P., 2016. Environmental
471 signal propagation in sedimentary systems across timescales. *Earth-Science Rev.* 153, 7–
472 29. doi:10.1016/j.earscirev.2015.07.012

473 Ryan, W.B.F., S.M. Carbotte, J.O. Coplan, S. O'Hara, A. Melkonian, R. Arko, R.A. Weissel, V.
474 Ferrini, A. Goodwillie, F. Nitsche, J. Bonczkowski, and R. Zemsky (2009), Global Multi-
475 Resolution Topography synthesis, *Geochem. Geophys. Geosyst.*, 10, Q03014,
476 doi:10.1029/2008GC002332.

477 Saucier, R.T. 1994. Geomorphology and Quaternary Geologic History of the Lower Mississippi
478 Valley. Mississippi River Commission, Vicksburg, MS.

479 Saucier, R.T. 1994. Geomorphology and Quaternary Geologic History of the Lower Mississippi
480 Valley. Mississippi River Commission, Vicksburg, MS.

481 Schwartz, T.M., Schwartz, R.K., Weislogel, A.L., 2019. Orogenic Recycling of Detrital Zircons
482 Characterizes Age Distributions of North American Cordilleran Strata. *Tectonics* 38, 4320–
483 4334. doi:10.1029/2019TC005810

484 Sharman, G.R., Sylvester, Z., Covault, J.A., 2019. Conversion of tectonic and climatic forcings
485 into records of sediment supply and provenance. *Sci. Rep.* 9, 1–7. doi:10.1038/s41598-019-
486 39754-6

487 Sharman, G.R., Sharman, J.P., Sylvester, Z., 2018. detritalPy : A Python - based toolset for
488 visualizing and analysing detrital geo - thermochronologic data 202–215.
489 doi:10.1002/dep2.45

490 Sickmann, Z.T., Chheda, T.D., Capaldi, T.N., Thomson, K.D., Paull, C.K., Graham, S.A., 2019.
491 Using provenance analysis in an Anthropocene natural laboratory. *Quat. Sci. Rev.* 221,
492 105890. doi:10.1016/j.quascirev.2019.105890

493 Sickmann, Z.T., Paull, C.K., Graham, S.A., 2016. Detrital Zircon Mixing and Partitioning in
494 Fluvial To Deep. *J. Sediment. Res.* 86, 1298–1307.

495 Sinha S. (2011) Sediment Routing. In: Singh V.P., Singh P., Haritashya U.K. (eds) *Encyclopedia*
496 *of Snow, Ice and Glaciers*. Encyclopedia of Earth Sciences Series. Springer, Dordrecht

497 Sømme, T.O., Helland-Hansen, W., Martinsen, O.J., Thurmond, J.B., 2009. Relationships
498 between morphological and sedimentological parameters in source-to-sink systems: a basis

499 for predicting semi-quantitative characteristics in subsurface systems. *Basin Res.* 21, 361–
500 387. doi:10.1111/j.1365-2117.2009.00397.x

501 Thomas, W.A., 2011. Detrital-zircon geochronology and sedimentary provenance. *Lithosphere* 3,
502 304–308. doi:10.1130/RF.L001.1

503 Thomson, K.D., Stockli, D.F., Clark, J.D., Puigdefàbregas, C., Fildani, A., 2017. Detrital zircon
504 (U-Th)/(He-Pb) double-dating constraints on provenance and foreland basin evolution of
505 the Ainsa Basin, south-central Pyrenees, Spain. *Tectonics* 36, 1352–1375.
506 doi:10.1002/2017TC004504

507 Vermeesch, P., 2013. Multi-sample comparison of detrital age distributions. *Chem. Geol.* 341,
508 140–146. doi:10.1016/j.chemgeo.2013.01.010

509 Weislogel, A.L., Graham, S.A., Chang, E.Z., Wooden, J.L., Gehrels, G.E., Yang, H., 2006.
510 Detrital zircon provenance of the Late Triassic Songpan-Ganzi complex: Sedimentary
511 record of collision of the North and South China blocks. *Geology*. doi:10.1130/G21929.1
512
513
514
515
516
517
518
519
520
521

522 **FIGURE CAPTIONS:**

523 **Figure 1. A:** Map of United States and portions of Canada showing major features discussed in
524 this paper, including the location of the Lower Mississippi Valley (modified from Rittenour et
525 al., 2007). **B:** Quaternary surficial geology and fluvial deposit ages of the Lower Mississippi
526 Valley, with sample locations discussed in this paper (modified from Rittenour et al. 2007;
527 Blum, 2019).

528
529 **Figure 2: A** lithostratigraphic column for Deep Sea Drilling Project (DSDP) Leg 96, Site 615
530 with detrital zircon samples from Fildani et al. (2018). MIS = marine isotope stage. SH = seismic
531 horizon. **B:** Proportions of U-Pb detrital zircon (DZ) ages from samples above and below seismic
532 horizon H-20. Note the systematic shift in young, western derived DZs above H-20.

533
534 **Figure 3. A:** Shaded elevation map of the central Mississippi alluvial Valley (GeoMapApp;
535 <http://www.geomapapp.org>; Ryan et al., 2009). **B, C:** Using a vibrocore device to sample buried
536 late Pleistocene sands at sample locations MV01 (25 ka) and sample location MV03. **D:** Bar
537 graph of sample bulk weight % and grain size for sands recovered from sample locations MV01
538 (blue) and MV03 (red).

539
540 **Figure 4.** Results of U-Pb detrital zircon (DZ) geochronology of bulk sediment samples
541 (captioned “bulk sed”), and sub samples from very fine (63 – 125 μm) and fine sand (125 – 250
542 μm) grain size fractions. Shown in the top panel are cumulative distribution functions (CDFs) for
543 each sample, with a color coded key to DZ source terranes of North America. Lower panels are
544 kernel density estimates (KDEs) displaying detrital age signatures of each sample and pie

545 diagrams with proportions keyed to the colors of the inset key. Lower case “n” = number of
546 individual U-Pb DZ ages per sample.

547

548 **Figure 5.** Cumulative distribution functions (CFs) and kernel density estimates (KDEs) for
549 amalgamated samples (= bulk sed + fine grain size + very fine grain sizes) from the late
550 Pleistocene Mississippi River, plotted with published DZ samples from modern large rivers of
551 the Mississippi system (Blum and Pecha, 2014), and plots of U-Pb DZ samples from late
552 Pleistocene (marine isotope stage 2) Mississippi deep-sea fan (Fildani et al., 2018). Pies color
553 coded to major North American zircon source terranes as in Figure 3.

554

555 **Figure 6. A, B:** Probability density plots for observed detrital zircon (DZ) samples from the
556 Western Lowlands (25 ka; MV01 amalgamated) and Eastern Lowlands (15 ka; MV03
557 amalgamated), expressed as bold black lines. Red bold line shows results of a forward mixture
558 model that distributes mixing weights equally across potential sediment sources, represented by
559 detrital zircon samples from modern tributaries to the Mississippi River (thin colored lines). **C,**
560 **D:** Probability density plots for observed DZ mixtures from the Western and Eastern Lowlands
561 (bold black lines) and best fit models (bold red lines) found by forward Monte Carlo simulations
562 (10⁶ iterations) of potential combinations of each parent tributary. Results reported as %
563 contribution to the downstream observed mixture.

564

565 **Figure 7.** Multidimensional scaling map (MDS map) for samples plotted in Figure 4. In this plot,
566 axes are unitless Euclidean distances that relate to sample similarity (See Vermeesch, 2013 for
567 explanation). Here, new detrital zircon samples from the late Pleistocene (marine isotope stage 2;

568 MIS-2; ~25 – 15 ka) Mississippi Valley samples plot closest to the age correlative deep-sea fan
 569 deposits, and also close to the modern Missouri River. See text for further explanation.

570

571 **Figure 8.** Google Earth satellite image of the lower Mississippi River Valley and interpreted
 572 ancient river courses. Pies are U-Pb detrital zircon (DZ) age signatures of samples from this
 573 study (MV01, MV03; 25 – 15 ka), and the DZ samples from the modern Missouri, Upper
 574 Mississippi, and Ohio Rivers, as well as the marine isotope stage 2 (MIS-2) deep-sea fan (~30 –
 575 12 ka).

576

Table 1: mixture model results

modern river sample	Western Lowlands ~25 ka	Eastern Lowlands ~15 ka
(parent component)	MV01 amalgamated (composite mixture)	MV03 amalgamated (composite mixture)
Ohio River	0%	2%
Upper Mississippi River	21%	13%
Missouri River	79%	80%
Arkansas River	0%	5%

577

578 **Table 1:** Results of unmixing detrital zircon samples from the Western Lowlands (amalgamated
 579 grain sizes and bulk sediment for MV01), and the Eastern Lowlands (amalgamated grain sizes
 580 and bulk sediment for MV03).

581

582

583

584

585

586

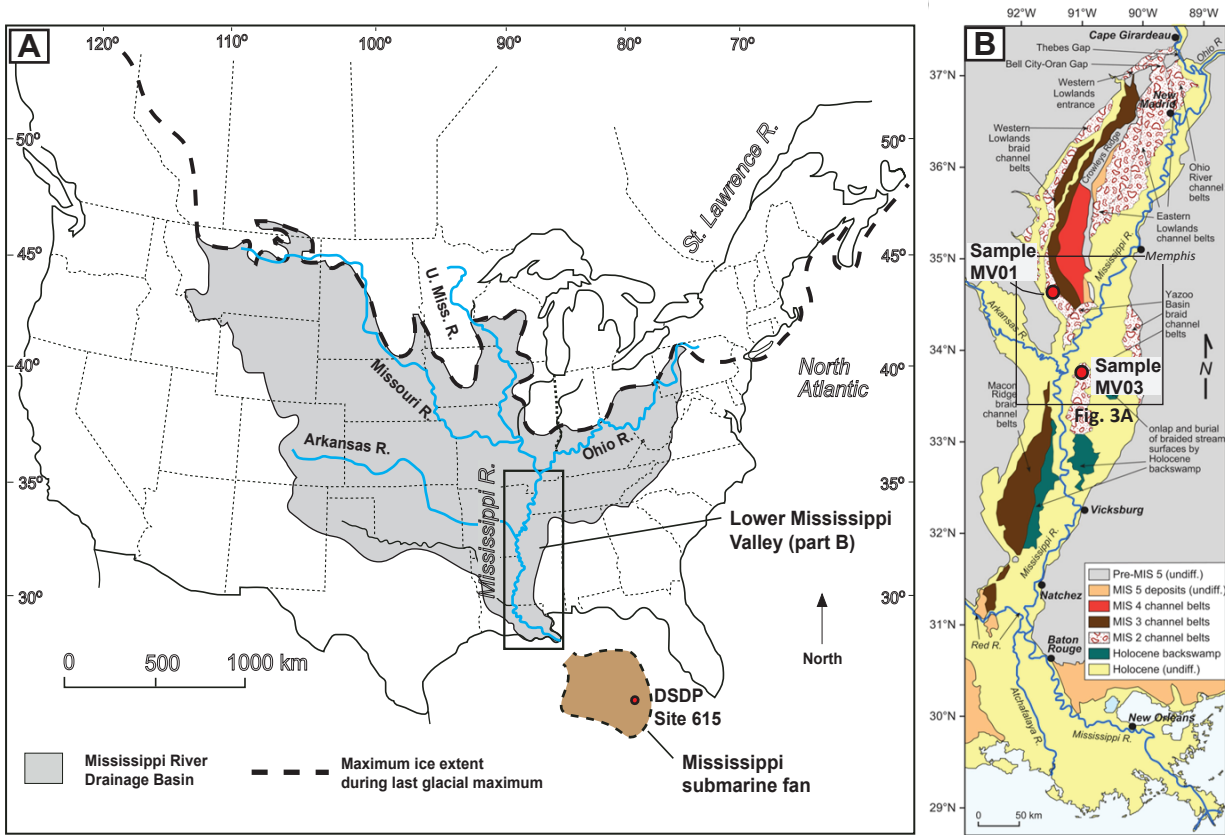


Figure 1 A and B

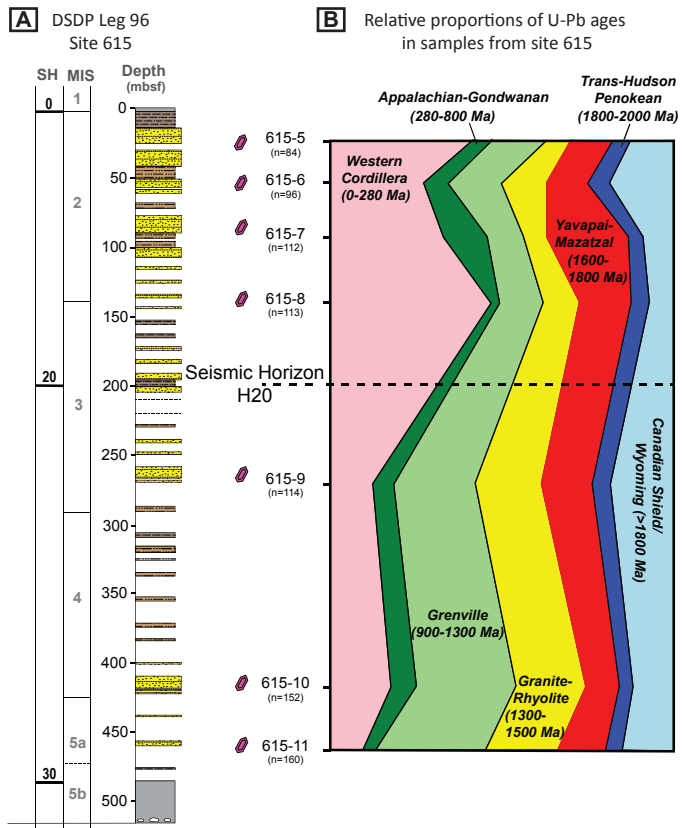
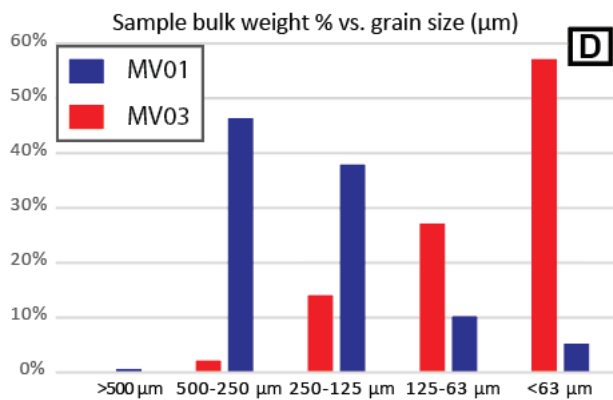
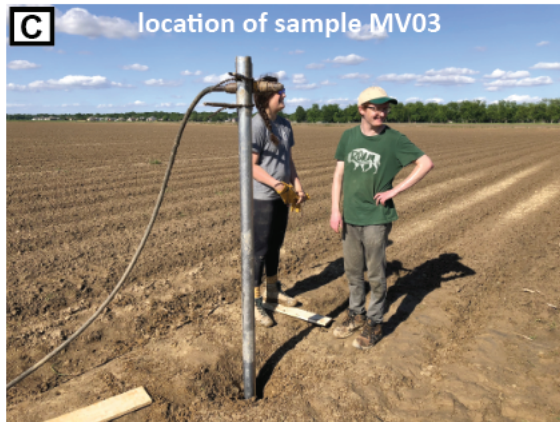
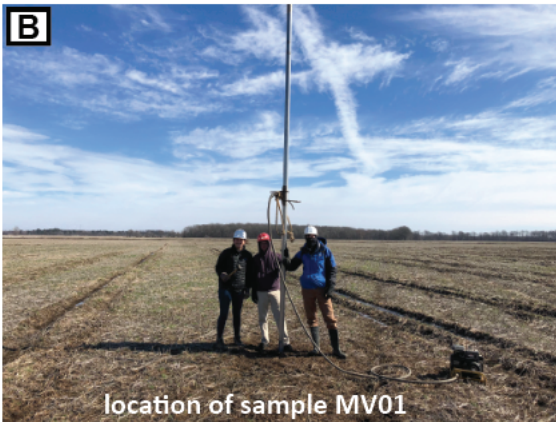
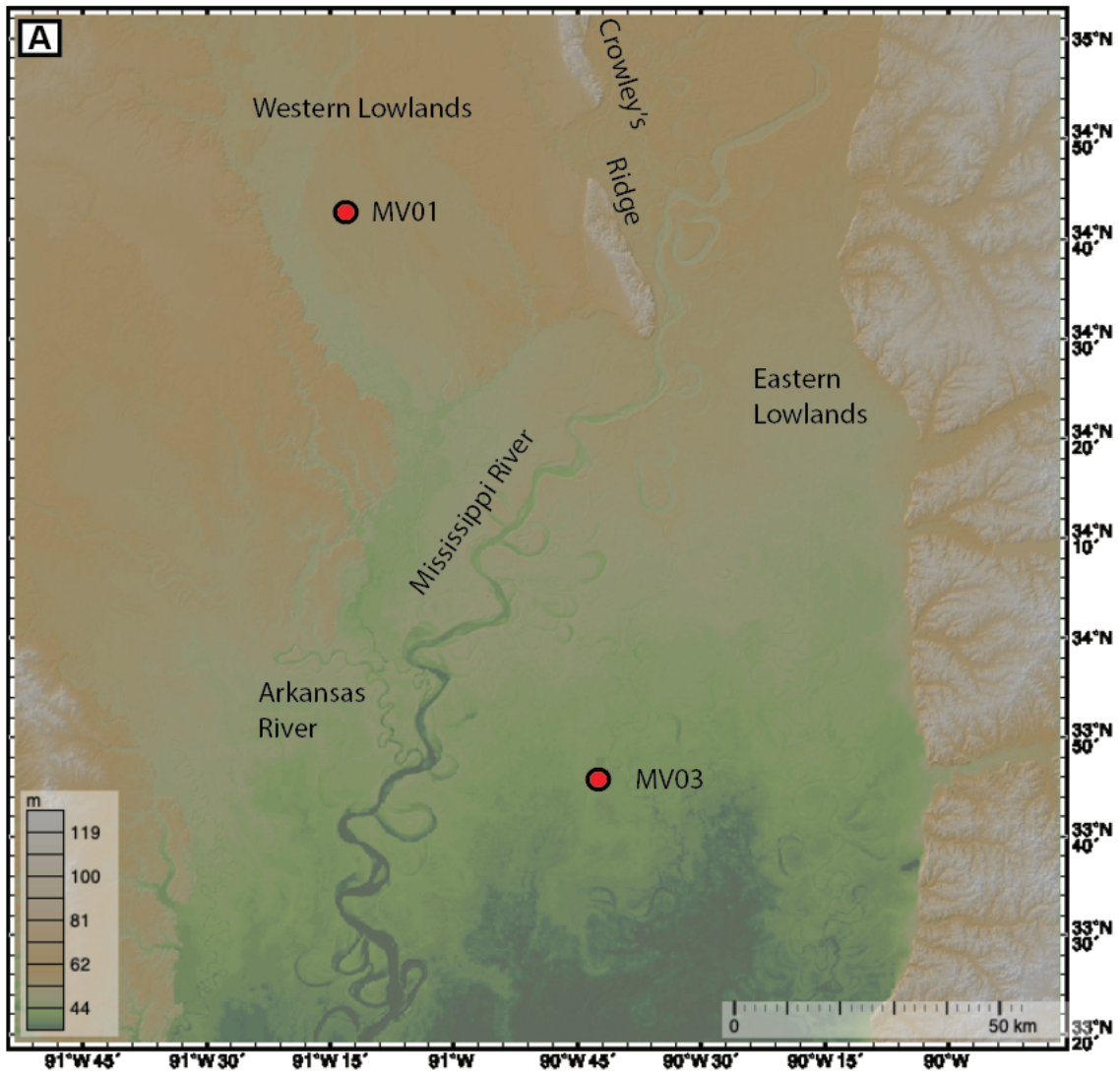


Figure 2 A-B



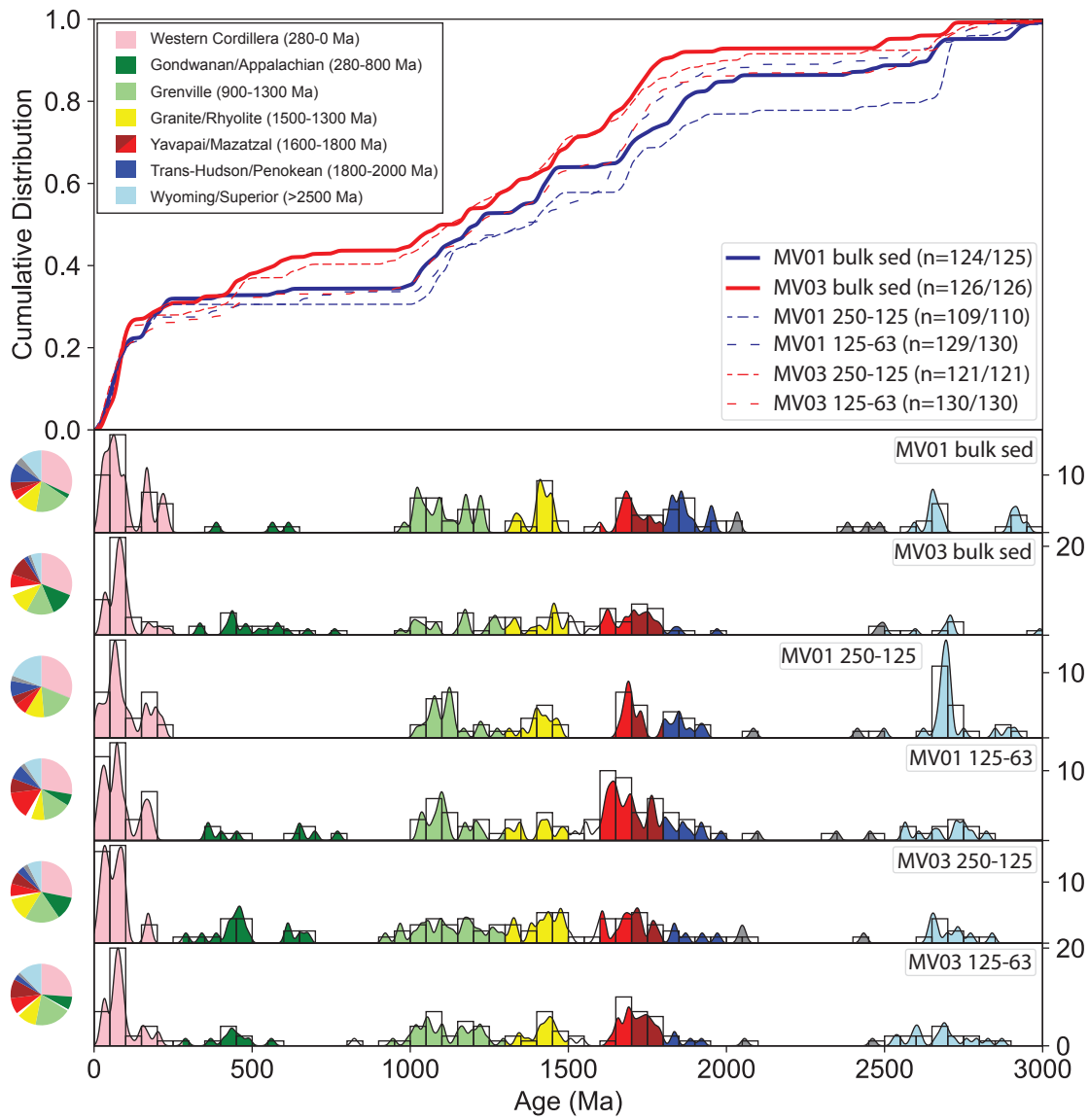


Figure 4

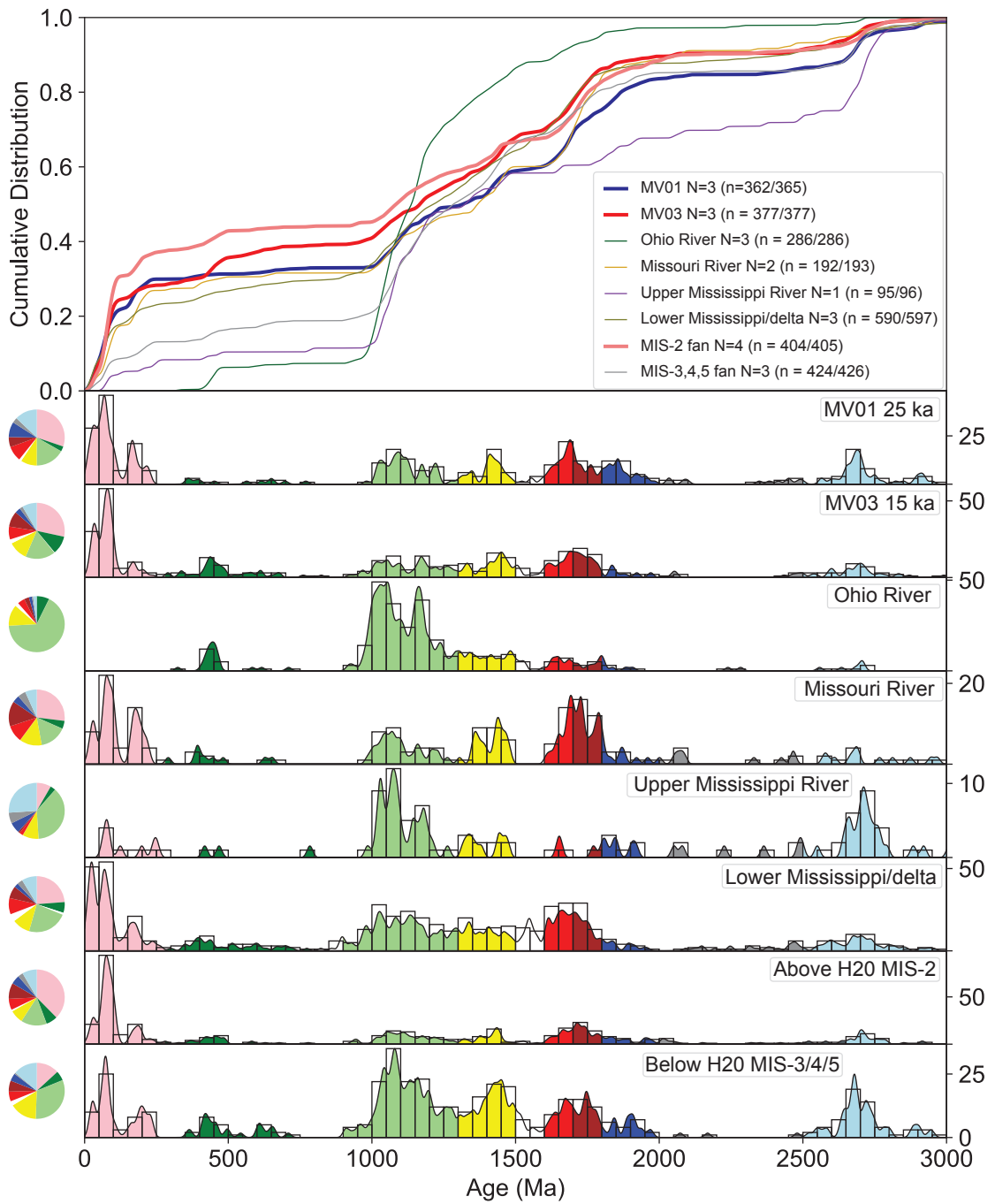


Figure 5

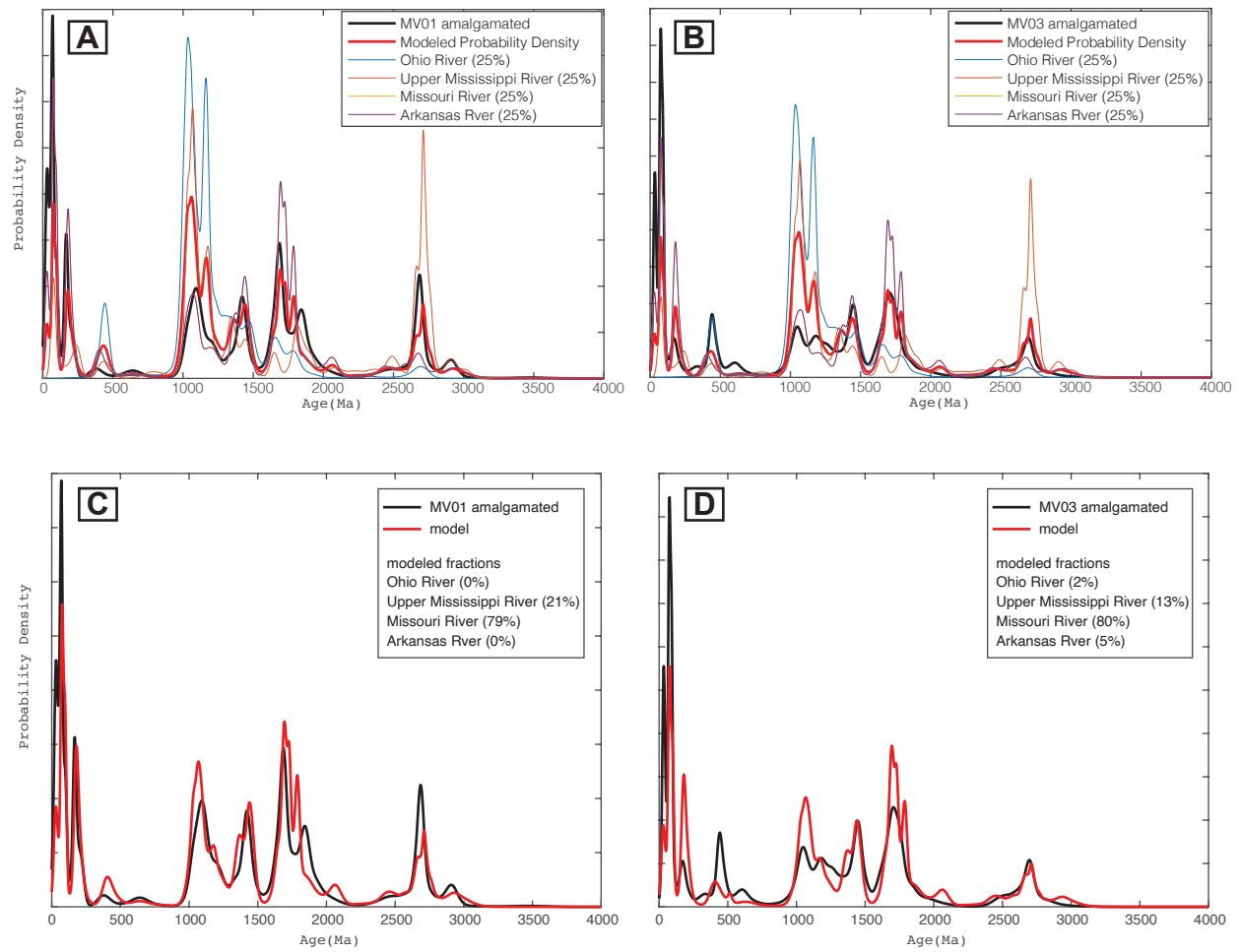


Figure 6 A-B-C-D

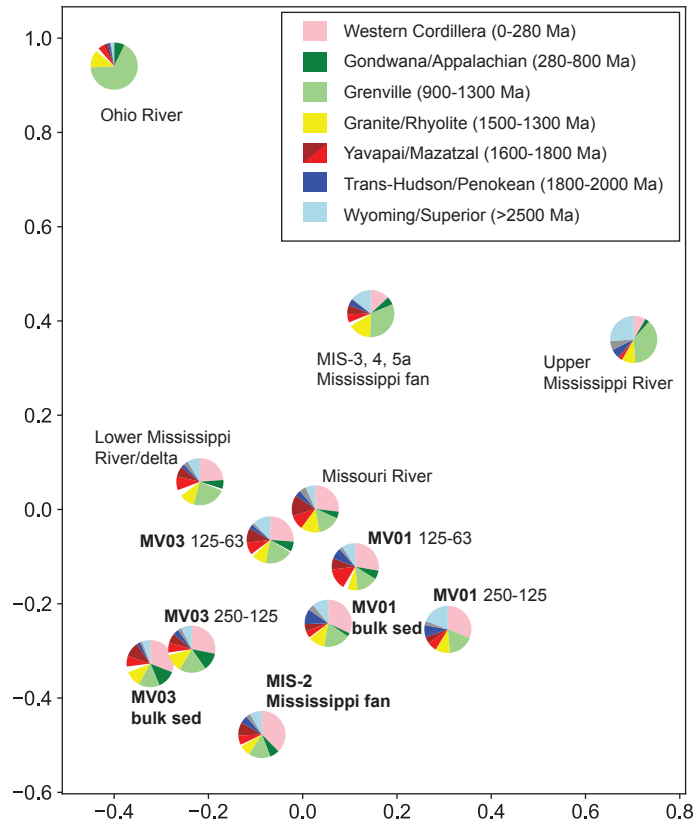


Figure 7

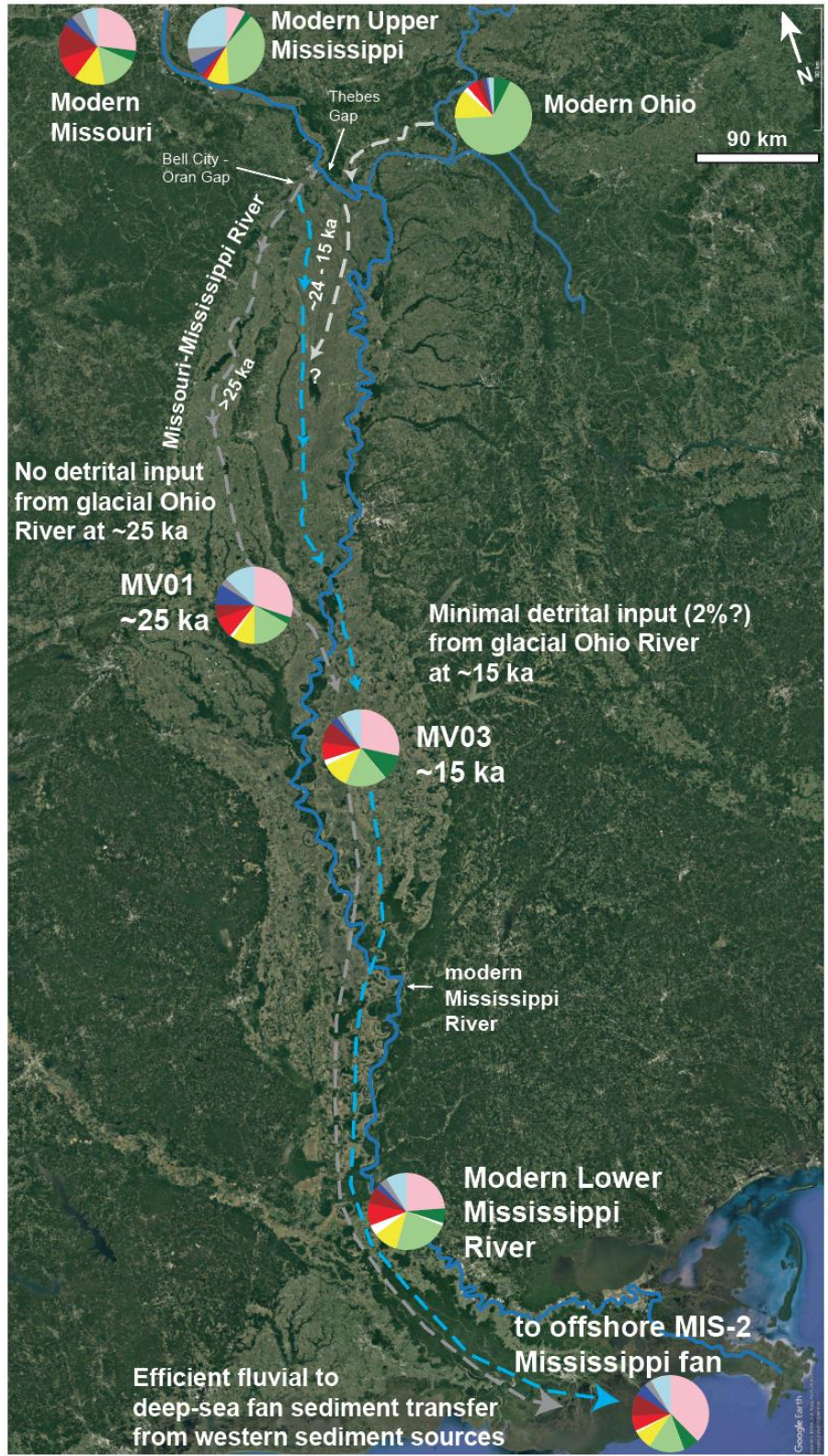


Figure 8